01 Jul 1994

Differential Transfer Ionization Cross Sections for 50175-keV Proton-Helium Collisions

S. W. Bross

S. M. Bonham

A. D. Gaus

Jerry Peacher
Missouri University of Science and Technology, peacher@mst.edu

et. al. For a complete list of authors, see https://scholarsmine.mst.edu/phys_facwork/1300

Recommended Citation

S. W. Bross et al., "Differential Transfer Ionization Cross Sections for 50175-keV Proton-Helium Collisions," *Physical Review A*, vol. 50, no. 1, pp. 337-342, American Physical Society (APS), Jul 1994.
The definitive version is available at https://doi.org/10.1103/PhysRevA.50.337

Differential transfer ionization cross sections for 50–175-keV proton-helium collisions

S. W. Bross, S. M. Bonham, A. D. Gaus, J. L. Peacher, T. Vajnai, and M. Schulz
Department of Physics and the Laboratory for Atomic and Molecular Research, University of Missouri-Rolla, Rolla, Missouri 65401

H. Schmidt-Böcking
Institut für Kernphysik, Universität Frankfurt, 6000 Frankfurt, Germany
(Received 19 November 1993; revised manuscript received 4 April 1994)

We have measured coincidences between neutralized projectiles and He recoil ions for 50–175-keV proton-helium collisions. From the data we obtained transfer ionization (TI) cross sections differential in the projectile scattering angle. Laboratory scattering angles range from 0 to 2.0 mrad. The experimental method allowed separation of the postcollision charge states of the target atoms. The ratio of the cross sections for TI to the sum of TI and single capture, F, is presented as a function of projectile scattering angle. Comparison is made to previous measurements of this ratio where data is available. The differential cross sections are compared to dynamical classical trajectory Monte Carlo (dCTMC) calculations. Agreement in the shape of the differential cross sections is good between the theory and measurement over the entire energy range.

PACS number(s): 34.50.Fa, 34.70.+e

INTRODUCTION

One of the most pressing questions in contemporary atomic-collision physics is that of the role of the electron-electron interaction in ion-atom collisions [1]. The proton-helium collision system is a particularly well-suited system to study the influence of the electron-electron interaction on the collision because there are only two electrons and the nuclear charges are small. A proton provides a well-localized (the De Broglie wavelength is very small for heavy ions at large collision energies), essentially structureless incident ion; whereas a bound electron has a position distribution described by the wave function and therefore is diffuse. The interaction of a structureless ion with a diffuse electron has been studied theoretically for some time. The effect of the interaction between two diffuse, bound electrons on ion-atom collisions, in contrast, presents a challenge to theory which has gained considerable interest in recent years.

In collision processes involving only one active electron (one-electron processes) the electron-electron interaction usually plays only a minor role. In collision processes involving two active electrons (two-electron processes), however, the electron-electron interaction can make a significant contribution and in some cases can even dominate the nuclear-electron interaction [2,3]. One such two-electron process, in which the electron-electron interaction is believed to be important, is transfer ionization (TI). In TI one of the target electrons is captured by the projectile, while a second target electron is ionized. The result of a transfer ionization event is thus a projectile with a reduced charge and a doubly charged target recoil ion. A pure capture process, in contrast, leads to a singly charged target recoil ion.

Horsdal, Jensen, and Nielsen [4] reported ratios of TI to charge transfer as a function of projectile scattering angle for projectile energies of 200–500 keV/amu. In these data pronounced peaks were observed at scattering angles around 0.5 mrad for all projectile energies. Horsdal, Jensen, and Nielsen [4] discussed Thomas scattering [5] of the second kind as a possible explanation for the enhancement in the ratio. In this type of scattering the projectile collides with one target electron which then undergoes a collision with another target electron. One electron leaves the collision region with the same velocity vector as the projectile and is subsequently captured. The second electron is ionized in this process. Due to kinematic constraints the projectile must be scattered at an angle of 0.55 mrad in this process, which could lead to an enhancement of the ratio at this angle. At higher collision energies Pálinkás *et al.* [6] found evidence of Thomas scattering [5] by measuring the ejected electrons in coincidence with the charge changed projectile. The observation of Horsdal, Jensen, and Nielsen [4] was nevertheless surprising because it was believed that the Thomas mechanism played only a minor role at collision energies as small as those studied by these authors.

Gayet and Salin [7] offered another explanation for the pronounced peaks in the data of Horsdal, Jensen, and Nielsen [4]. They make the same arguments as those made earlier by Dörner *et al.* [8] to describe similar effects observed in the double-to-single ionization ratios [9]. In this model the structures in the data can be understood by assuming that both electrons are independent; that is, the electron-electron interaction is neglected. In the work of Gayet and Salin [7] the structure in the differential cross section is interpreted as a manifestation of a different slope structure in the angular dependence of the single-capture and transfer ionization differential cross sections. A change of slope in these differential cross sections occurs because of the different regions probed by the projectile in the collision. At large impact parameters the projectile is mainly deflected due to an interaction with the target electrons, and deflection due to an interaction with the target nucleus is negligible. At

comparatively small impact parameters, in contrast, the projectile penetrates the electron cloud and is primarily deflected by an interaction with the target nucleus. Single capture requires only one interaction between the target electron and the projectile. Since the maximum scattering angle for a proton deflected by a free electron is approximately 0.55 mrad, only deflections from the target nucleus can lead to projectile scattering angles larger than 0.55 mrad. Transfer ionization, in contrast, requires two projectile electron interactions. The scattering of the projectile off two target electrons can contribute to scattering angles as large as 1.1 mrad. Consequently, there is a change of slope at approximately 0.55 mrad in the single-capture differential cross sections, and at approximately 1.1 mrad in the transfer ionization differential cross sections. With these changes of slope in the differential cross sections, Gayet and Salin [7] demonstrated that it is possible to obtain a pronounced peak in the TI-to-single-capture ratios around 0.5 mrad.

The experiment detailed here reports the relative magnitudes of the processes that lead to the removal of one or both electrons from a helium atom in capture collisions with a proton. Specifically this experiment measures the ratios F of the cross section for TI to the sum of the cross sections for TI and single capture. The ratios were studied for collision energies of 50, 100, and 175 keV. This energy range corresponds to velocities for the proton ranging from 1.41 to 2.65 a.u.. This velocity range corresponds roughly to the orbital velocities of the helium ground-state electrons. The velocity matching of the projectile and the target electrons makes a theoretical treatment of the collision challenging because the collisions are too slow for perturbative approaches and too fast for molecular treatments.

EXPERIMENT

Data for the present work were acquired using the 200-kV accelerator which is part of the University of Missouri-Rolla ion energy-loss spectrometer. Details of the operation of the machine have been given elsewhere [10], and only the salient points of the present arrangement are described here. The experimental setup is shown in Fig. 1. Protons are created by dissociating H_2 in a microwave discharge. Ions are extracted from the plasma by a constant potential, and the protons are selected by a Wien filter. The protons are then accelerated to energies of 50, 100, and 175 keV. The beam is collimated by two sets of precollision slits, then steered through the optical axis of the scattering center. After leaving the collision region, projectiles that were neutralized in the collision pass undeflected through a switching magnet which sweeps out projectiles that did not charge change. The charge-changed projectiles (neutral hydrogen) pass through a set of solid angle-defining slits and are detected by a focused-mesh electron multiplier. The target region consists of a gas spritzer placed between a set of parallel plates. A voltage is applied to the plates to extract singly and doubly charged helium recoil ions produced in the collisions. The recoil ions accelerate and pass through a grid on one of the parallel plates into a drift region that is maintained at a constant potential. In this region the differently charged recoil ion species drift apart due to the different velocities obtained in the acceleration region. Upon exiting the drift region the recoil ions are attracted by a negative potential applied to the front of a continuous dynode electron multiplier. The output signal of the recoil detector is sent through a delay generator and used as the stop signal for a time-to-digital converter (TDC). The output signal from the neutral detector is used to start the TDC conversion. The TDC output signals and the total neutral projectile and recoil ion count rates were recorded. A target pressure dependence was taken and found to be linear for the He^e coincidences, to ensure that the target gas density was well below the region where double collisions occur. The recoil extraction field (150 V/cm) was sufficiently large to ensure that all recoil ions were collected. A further increase in voltage did not lead to an increase in the recoil rate.

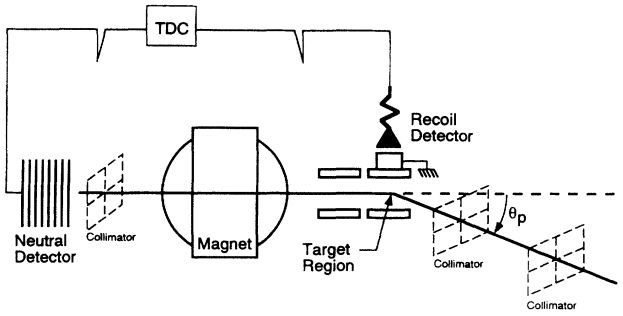

FIG. 1. Schematic of the experimental setup. Protons are incident from the right at an angle θ_p. The neutralized projectiles pass through the switching magnet and the solid angle defining slits to create the start pulse for the time-to-digital converter. Recoil ions created in the target region are extracted and create the stop pulse for the TDC.

A profile of the incident beam was acquired with no target gas. This serves two purposes: the beam can be checked for angular asymmetries; and the profile, which determines the angular divergence of the incident beam, is later used to deconvolute the effects of the apparatus geometry from the angular differential cross sections. The angular resolution was 0.2-mrad full width at half maximum (FWHM). The zero-scattering angle is determined from the true proton-helium coincidences. Target gas is admitted to the collision region and the single-channel analyzer (SCA) of a time-to-amplitude converter (TAC) is used to record counts as a function of scattering angle for single-capture events. As the single capture differential cross section is strongly peaked in the forward direction, this allows for an accurate determination of the zero-scattering angle by maximizing the SCA count rate as a function of scattering angle.

After the determination of the zero-scattering angle, multiple-angle data sets were acquired at a given energy by cycling through several preset angles. The scattering angles were scanned by rotating the accelerator around the center of the target region. The total recoil count

rate was recorded for each angle for normalization. Zero positions were frequently checked both before and after data runs with no deviation of zero positions discovered within experimental uncertainties. We also took integral coincidence time spectra at all collision energies with the solid angle-defining slits taken out. Using time-of-flight techniques to separate the recoil ion charge states and coincidence techniques to correlate recoil ions with charge-changed projectiles allows the simultaneous measurement of He^+ and He^{2+} ions at each projectile-scattering angle.

RESULTS AND DISCUSSION

An example of a coincidence time spectrum is shown in Fig. 2 for zero projectile-scattering angle and an incident proton energy of 50 keV. The time resolution of approximately 20 ns was sufficient to separate the various recoil ion species. The recoil ion species which can be identified are H^+, He^+, He^{2+}, and HO^+. The time of flight of the recoil ion is proportional to the square root of its mass-to-charge ratio. In Fig. 3 we show a plot of the time of flight as a function of this parameter along with a straight-line fit. The linear dependence indicates a correct assignment of the ion species in the coincidence spectrum. With the target gas removed, no peaks were observed in either the He^+ or He^{2+} positions in the time spectrum. The H^+ and HO^+ peaks were still present, and are due to residual water vapor in the vacuum system. Due to the low TDC stop rates (neutral species), the random coincidence rate exhibits a straight, flat time dependence. To extract the true coincidence count rates for each recoil ion species, a random coincidence region was chosen from each spectrum and fit with a straight line. This line was used to subtract the random counts from the region of the peaks. After background subtraction it is straightforward to obtain the ratios F defined above.

The values obtained for the integral ratio (obtained with the solid angle-defining slits taken out) agree well with the previously reported values of Kristensen and Horsdal [11] at all energies. A comparison of the two

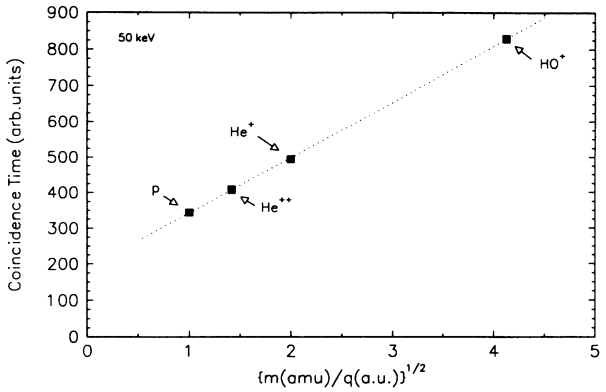

FIG. 3. Plot of the coincidence time vs the square root of the mass to charge ratio of the recoil ions. The linear dependence indicates a correct assignment of the recoil ion species to the time peaks in Fig. 2.

sets of integrated ratios taken from Ref. [11] shows that the total ratios taken from Kristensen and Horsdal are approximately 10% lower than the results of Horsdal-Pedersen and Larsen [12] over the energy range covered. The ratios computed from the total cross sections of Shah and Gilbody [13,14] tend more toward the data of Horsdal-Pedersen and Larsen [12].

The differential ratios for the three energies considered in this work are shown in Figs. 4–6. It should be noted that these ratios are essentially free of systematic errors due to uncertainties in detector efficiencies, target pressure, beam intensity, etc. because both the TI and single-capture events were recorded simultaneously with the same detector system. Therefore, these potential sources of systematic errors cancel in the ratios. If, on the other hand, the TI and single-capture cross sections are measured in separate experiments and the ratios calculated from those results, the error will be substantially greater because of the error propagation from both cross sections. Therefore, reliable ratios can only be determined by measuring the TI and single-capture events simultaneously.

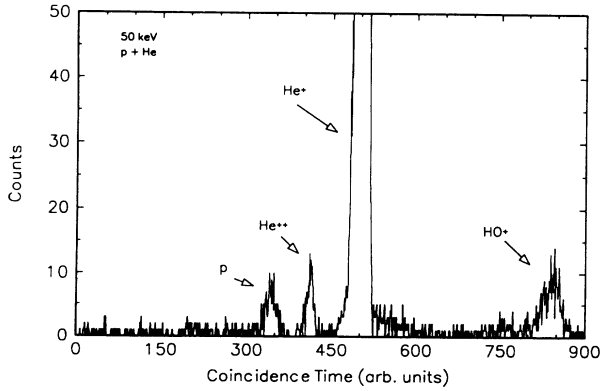

FIG. 2. A coincidence time spectrum taken for a collision energy of 50 keV and a scattering angle of 0°. Besides the He^+ and He^{2+} recoil ions, protons and HO^+ ions can be identified which are due to water vapor in the residual gas.

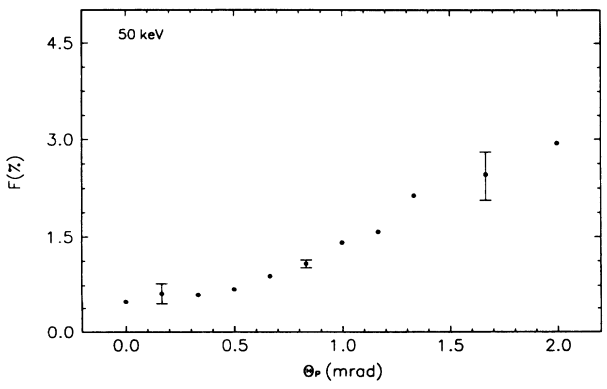

FIG. 4. The ratio of the transfer ionization to total capture events as a function of the laboratory scattering angle for a 50-keV proton-helium collision. Error bars represent the standard deviation of the mean from all the data sets.

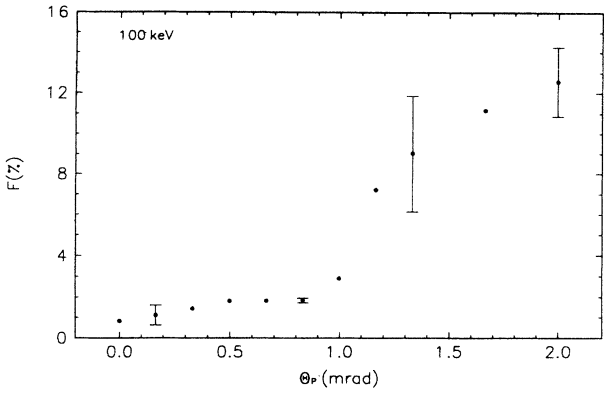

FIG. 5. Same as Fig. 4 for 100 keV.

Our data for the differential ratio at 50 keV show a monotonic increase with laboratory scattering angle. The 100-keV data exhibit the same behavior out to approximately 0.9 mrad where a sharp increase in the value of the ratio occurs. After the increase, the 100-keV ratio appears to level out against laboratory scattering angles around 2 mrad. The 100-keV data can be compared to the data of Kristensen and Horsdal [11] for a projectile laboratory scattering angle of 2 mrad. Our value for the ratio at this energy and laboratory scattering angle of 12.5% agrees almost exactly with the value reported by Kristensen and Horsdal.

The 175-keV data exhibit a similar peak structure as that seen by Horsdal, Jensen, and Nielsen [4]. However, in the present work the peak structure is shifted out in angle to about 0.9 mrad as compared to the data of Horsdal, Jensen, and Nielsen [4]. This shift does not necessarily indicate an inconsistency between our data and those of Horsdal, Jensen, and Nielsen. A closer inspection of the work of Horsdal, Jensen, and Nielsen reveals that at 200 keV the peak is also shifted compared to the larger collision energies and occurs at about 0.7 mrad. Our data at 175 keV may thus be taken as an indication of a systematic shift of the peak with decreasing collision energies to larger scattering angles, until it disappears at some collision energy between 100 and 175 keV.

The interpretation by Horsdal, Jensen, and Nielsen of the peak structure as a manifestation of the Thomas scattering mechanism is based on kinematic effects in the collision. On the other hand, any mechanism which is nearly independent of the collision kinematics could conceivably lead to large differences in the angular dependence of the TI-to-single-capture ratios as a function of the projectile energy. Such a collision energy dependence can be produced artificially when certain parameters are determined as a function of scattering angle, since the relation between impact parameter and scattering angle is collision energy dependent. In order to avoid this problem, we show in Fig. 7 the values for F as a function of impact parameter for all collision energies. The impact parameter was determined using an unscreened Coulomb potential. For large impact parameters the values one would obtain for a more realistic, screened potential could be significantly smaller than those we are using. However, for impact parameters smaller than the K-shell radius of the He atom (≈ 0.75 a.u.), screening should not have a large effect. Here we use only the impact parameter dependence to qualitatively discuss to what extent the ratios F are affected by kinematic effects.

The data for F for all three collision energies follow a universal curve within experimental uncertainties as a function of the impact parameter. These ratios thus appear to be nearly independent of kinematic effects. The interpretation of the peak structure in the data of Horsdal, Jensen, and Nielsen as due to either the Thomas

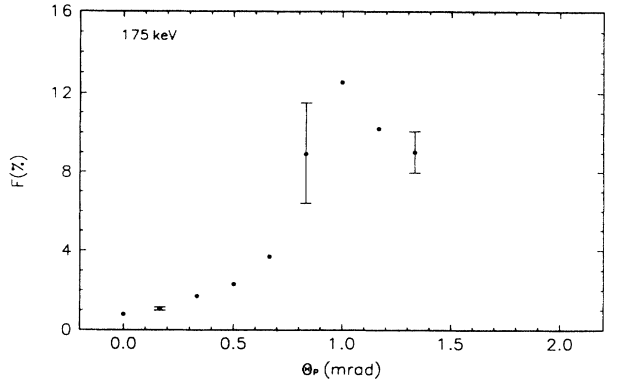

FIG. 6. Same as Fig. 4 for 175 keV.

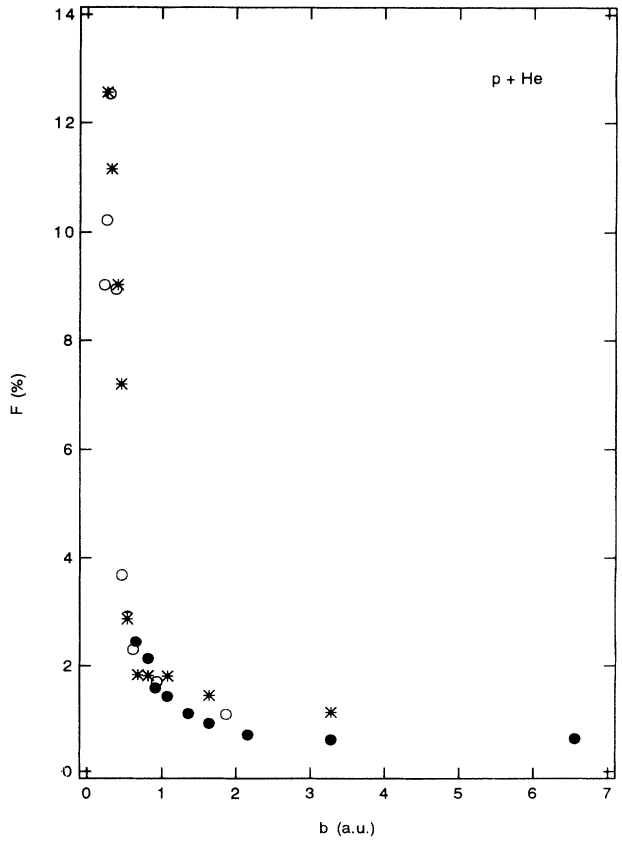

FIG. 7. The ratio of transfer ionization to total capture as a function of the impact parameter. The full circles are the data for 50 keV, the stars for 100 keV, and the open circles for 175 keV.

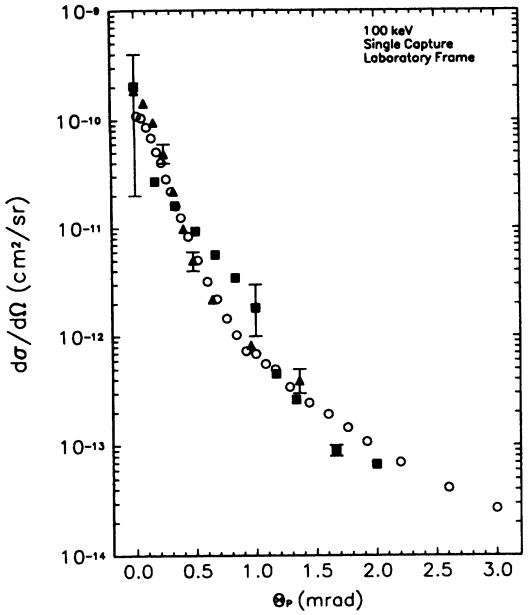

FIG. 8. Differential single-capture cross sections as a function of laboratory scattering angle for 100-keV $p+$He. The squares are the experimental data of this work, the triangles are experimental data from Martin *et al.* [10], and the open circles show a dCTMC calculation by Meng and Olson [15].

scattering or the independent electron model of Gayet and Salin is based on kinematic effects. It is therefore not clear that our data can be explained by either approach. However, the peak structure in the data of Horsdal, Jensen, and Nielsen appears at the same scattering angle for collision energies of 300 keV and larger, which means that the corresponding impact parameters differ. Thus at these higher collision energies the peak structure appears to be due to kinematic effects.

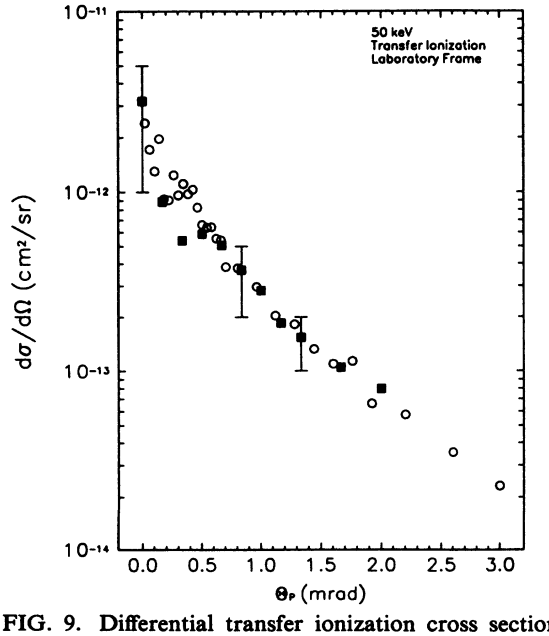

FIG. 9. Differential transfer ionization cross sections as a function of laboratory scattering angle for 50-keV $p+$He. The squares are the experimental data, the open circles show a dCTMC calculation by Meng and Olson [15].

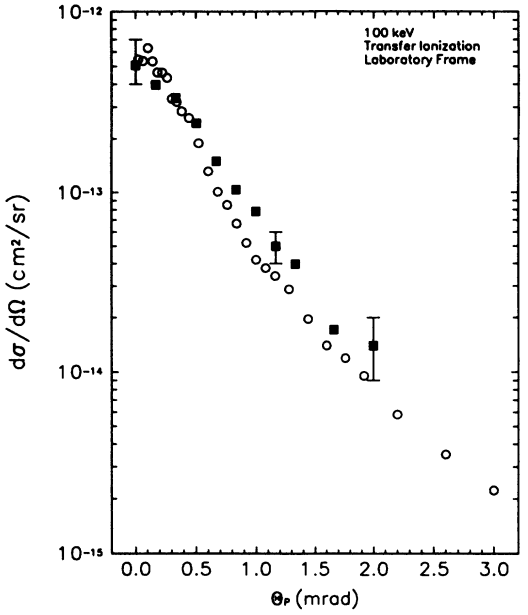

FIG. 10. Same as Fig. 9 for 100 keV.

We have determined the differential TI cross sections from our data. We also determined the differential single-capture cross sections from our data in order to compare with the results of Martin *et al.* [10] as a consistency check of our data. We normalized our integrated cross sections to the same total cross section as Martin *et al.* did. This comparison is shown for 100 keV in Fig. 8. Our results are consistent within experimental errors with the results of Martin *et al.* In Figs. 9–11 we show the differential TI cross sections as a function of laboratory scattering angle for 50-, 100-, and 175-keV collision energies, respectively. The absolute magnitude of these cross sections was obtained by integrating the relative

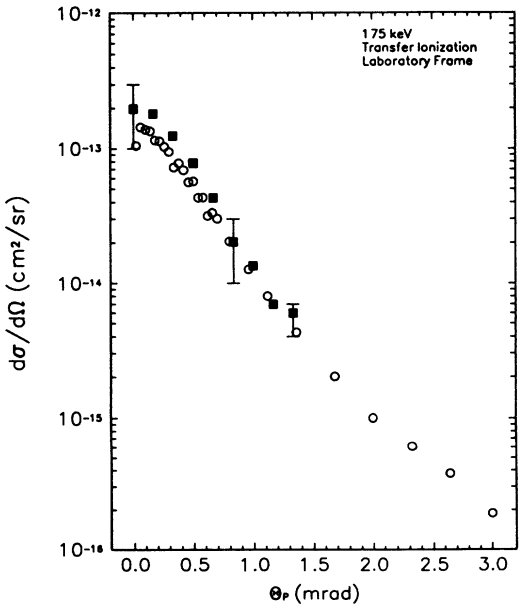

FIG. 11. Same as Fig. 9 for 175 keV.

differential cross sections over all scattering angles and normalizing these to the total TI cross sections of Shah and Gilbody [13,14]. If, instead of normalizing to total cross sections, the absolute differential TI cross sections are determined as a product of our differential single-capture sections and the ratios F of Figs. 4–6, the cross sections are about 40% smaller than those of Figs. 9–11 for all scattering angles. As pointed out above, the errors in the absolute cross sections are significantly larger than in the ratios. Therefore, the ratios provide much more reliable information. The open circles in Figs. 9–11 represent dCTMC calculations [15]. The calculations were also normalized to the total cross sections of Shah and Gilbody [13,14]. The experimental data demonstrate good agreement in shape with the dCTMC calculations. The 50-keV calculation results show very good agreement in slope over the entire angular range with the experimental data. At 100 keV there is fair agreement; however, the experimental data appear to show a somewhat flatter angular dependence than the calculation. At very small scattering angles the calculation is slightly lower than the experimental data and higher at larger angles. The 175-keV calculation results show good agreement in slope over the range of the experiment, with the experimental data exhibiting slightly higher values at the small scattering angles.

CONCLUSION

We have studied transfer ionization (TI) and single capture in $p+$He collisions at collision energies of 50, 100, and 175 keV. For 175 keV the ratios of the TI cross sections to the sum of TI and single-capture cross sections as a function of scattering angle exhibit a peak structure similar to those observed by Horsdal, Jensen, and Nielsen [4] at higher collision energies. At 50 and 100 keV such peak structures are not observed. If these ratios are plotted as a function of the impact parameter, the data for all collision energies studied in the present work fall on a universal curve within experimental uncertainties. This indicates that at these collision energies the mechanism leading to TI is nearly independent of kinematic effects. The angular differential TI cross sections are in good agreement with a dCTMC calculation by Meng and Olson [15].

ACKNOWLEDGMENTS

We would like to thank Dr. R. E. Olson and Dr. L. Meng for making the results of their calculation available to us prior to publication. This work was supported by the National Science Foundation Grant No. 9020813. One of us (H.S.B.) acknowledges support by NATO.

[1] J. H. McGuire, Adv. At. Mol. Opt. Phys. **29**, 217 (1992).
[2] J. A. Tanis, E. M. Bernstein, W. G. Graham, M. P. Stöckli, M. Clark, R. H. McFarland, T. J. Morgan, K. H. Berkner, A. S. Schlachter, and J. W. Steams, Phys. Rev. Lett. **53**, 2551 (1984).
[3] M. Schulz, E. Justiniano, R. Schuch, P. H. Mokler, and S. Reusch, Phys. Rev. Lett. **58**, 1734 (1987).
[4] E. Horsdal, B. Jensen, and K. O. Nielsen, Phys. Rev. Lett. **57**, 1414 (1986).
[5] L. H. Thomas, Proc. R. Soc. London **114**, 561 (1927).
[6] J. Pálinkás, R. Schuch, H. Cederquist, and O. Gustafsson, Phys. Rev. Lett. **63**, 2464 (1989).
[7] R. Gayet and A. Salin, Nucl. Instrum. Methods B **56**, 82 (1991).
[8] R. Dörner, J. Ullrich, H. Schmidt-Böcking, and R. E. Olson, Phys. Rev. Lett. **63**, 147 (1989).
[9] J. P. Giese and E. Horsdal, Phys. Rev. Lett. **60**, 2018 (1988).
[10] P. J. Martin, K. Arnett, D. M. Blankenship, T. J. Kvale, J. L. Peacher, E. Redd, V. C. Sutcliffe, J. T. Park, C. D. Lin, and J. H. McGuire, Phys. Rev. A **23**, 2858 (1981).
[11] F. G. Kristensen and E. Horsdal, J. Phys. B **23**, 4129 (1990).
[12] E. Horsdal-Pedersen and L. Larsen, J. Phys. B **24**, 4085 (1979).
[13] M. B. Shah and H. B. Gilbody, J. Phys. B **18**, 899 (1985).
[14] M. H. Shah and H. B. Gilbody, J. Phys. B **22**, 3037 (1989).
[15] L. Meng and R. E. Olson (private communication).